J Wood Sci (2007) 53:442–448
DOI 10.1007/s10086-007-0879-7

ORIGINAL ARTICLE

Kengo Ishimaru · Toshimitsu Hata · Paul Bronsveld
Takashi Nishizawa · Yuji Imamura

Characterization of sp^2- and sp^3-bonded carbon in wood charcoal

Received: October 19, 2006 / Accepted: January 15, 2007 / Published online: July 9, 2007

Abstract Japanese cedar (*Cryptomeria japonica)* preheated at 700°C was subsequently heated to 1800°C and characterized by electron microscopy, X-ray diffraction, and micro-Raman spectroscopy. The degree of disorder of carbon crystallites and the amount of amorphous phase decreased considerably with an increase in heat treatment temperature to 1400°C, while carbon crystallites clearly developed above this temperature, showing that the microstructure of carbonized wood undergoes drastic changes around 1400°C. Besides showing the bands for sp^2-bonded carbon, the Raman spectra showed a shoulder near 1100 cm^{-1} assigned to sp^3-bonded carbon. With an increase of heat treatment temperature, the peak position of the Raman sp^3 band shifted to a lower frequency from 1190 to 1120 cm^{-1}, which is due to the transformation of sp^3-bonded carbon from an amorphous phase to a nanocrystalline phase. These data showed that the microstructure of carbonized wood from 700° to 1800°C consisted of the combination of sp^2- and sp^3-bonded carbon, which is probably due to the disordered microstructure of carbonized wood. It is suggested that the sp^3-bonded carbon is transformed from an amorphous structure to a nanocrystalline structure with the growth of polyaromatic stacks at temperatures above 1400°C.

Key words Charcoal · Carbonization · Microstructure · Raman spectroscopy

K. Ishimaru (✉)
Daiwa House Industry Co. Ltd., 6-6-2 Sakyo, Nara 631-0801, Japan
Tel. +81-74-270-2146; Fax +81-74-272-3062
e-mail: k-ishimaru@daiwahouse.jp

T. Hata · Y. Imamura
Research Institute for Sustainable Humanosphere, Kyoto University, Uji 611-0011, Japan

P. Bronsveld
Department of Applied Physics, University of Groningen, 9747 AG Groningen, the Netherlands

T. Nishizawa
Polymer Electrolyte Fuel Cell Cutting-Edge Research Center, National Institute of Advanced Industrial Science and Technology, Tokyo 135-0064, Japan

Introduction

Carbon materials are classified in terms of their graphite-related and diamond-related carbon structures. The former is composed of stacking hexagonal carbon layers based on sp^2-bonded carbon atoms; the latter consists of sp^3-bonded carbon atoms involved in a tetrahedral bonding geometry. The microstructure of graphite-related carbon materials consists mainly of carbon crystallites, cross-linking between them, and oxygen-containing functional groups. It is suggested that the carbon crystallites are combined by cross-linkings such as sp^3-bonded carbons.[1,2] We have previously reported that the sp^3-bonded carbon such as nanodiamond in addition to sp^2-bonded carbon are formed in wood during the carbonization process.[3] The qualification of sp^3-bonded carbon in carbonized wood has, however, been rarely discussed.

The physicochemical properties of carbon materials are dominated by the nature of the microstructure. Without detailed microstructural knowledge, optimization of the processing and properties of wood-based carbon materials is extremely difficult. The recent developments in wood-based carbon materials provide new application fields for the new functions of carbonized wood such as catalytic graphitization and SiC composites, while at the same time demonstrating the necessity of finding a way to control its microstructure.[4–7] The further development of various wood-based carbon materials requires that the carbonization process of wood and the formation mechanism of the microstructure in carbonized wood be sufficiently clarified, and that their microstructure on the nanoscale be fully controlled. However, there are few studies of the microstructural changes in carbonized wood that accompany the completion of carbonization at heat treatment temperature between 1000° and 2000°C.[5,8–12]

In the present study, the structural changes of sp^2- and sp^3-bonded carbon in carbonized wood with an increase of heat treatment temperature from 700° to 1800°C were characterized in detail by transmission electron microscopy

(TEM), X-ray diffraction (XRD), and micro-Raman spectroscopy.

Experimental

Wooden blocks of Japanese cedar (*Cryptomeria japonica*) with dimensions of approximately 20 (L) × 12 (R) × 12 (T) mm and organosolve lignin powder (passing 200 mesh, Alcell Technologies) dried at 105°C for 24 h were heated to 700°C with a heating rate of 4°C/min in a laboratory-scale electric furnace. The temperature was kept constant for 1 h in a N_2 gas flow and then cooled to room temperature. After putting the sample heated at 700°C in a graphite mold, it was heated from room temperature to target temperatures of 1200°, 1400°, 1600°, and 1800°C at a heating rate of 15°C/min and the temperature kept constant for 30 min in a current-heating device (Plasman, SS Alloy, Hiroshima) under vacuum.[7] Lignin powder preheated at 700°C was heated to only 1800°C. An electric current was applied directly to the sample through a graphite die.

Crystalline phase characterization was conducted by conventional X-ray diffraction techniques (RINT-ultraX18 diffractometer) on samples using 40 kV/150 mA CuKα radiation. TEM samples were powdered by hand in an agate mortar. The powder was dispersed in isopropyl alcohol, which was spread over a lacy carbon grid for observation in a Jeol JEM-200EXII microscope operating at 100 kV.

Raman spectra of the carbonized samples were recorded at room temperature with a Renishaw inVia Raman spectroscope equipped with an air-cooled CCD detector. An argon laser (λ = 514.5 nm) was adopted as an excitation source and was focused to approximately 1 μm in diameter at a power of less than 1 mW at the sample surface. The Raman spectra were recorded more than three times for each analysis point in order to check sample damage by laser irradiation and at three different points on a sample under the same measuring condition to avoid spurious changes in spectral intensities. All Raman spectra were measured in the 1000–1800 cm^{-1} zone and fitted using five Gaussian/Lorentzian curves. The wavenumber was calibrated using the 520 cm^{-1} line of a silicon wafer.

Results and discussion

From TEM observation of the cell wall sections of wood carbonized at 700° and 1800°C, the predominant microstructure had a turbostratic nature that showed random orientation of the carbon crystallites.[12] In this article, we first discuss the microstructural change of wood carbonized from 700° to 1800°C according to observations made by TEM. Figure 1 depicts several 002 dark field (DF) TEM images of carbonized samples heat-treated at different temperatures. At 700°C, at the early stage of carbonization, the sample has a turbostratic nature, as was observed by Huttepain and Oberlin.[13] The 002 DF image (Fig. 1a) shows many small bright domains attributed to microcarbon crystallites made of layers of hexagonal sp^2-bonded carbon.[13] The degree of order in carbon crystallites was low and there was no trace of any preferential orientation in the sample.[13] In the 002 DF images obtained at 1200° and 1400°C, clusters made of a few bright domains were scattered among small bright dots as shown in Fig. 1b, c. At 1600°C, many clusters of bright domains of carbon crystallites are observed in the 002 DF image (Fig. 1d). At 1800°C, the large clusters of carbon crystallites were dominant in the sample (Fig. 1e). Thus, it is obvious that the carbon crystallites grow remarkably at temperatures over 1400°C.

XRD patterns of carbonized wood are shown in Fig. 2. Diffraction from the 002 planes ($2\theta = 26°$), the overlapping 100 and 004 planes ($2\theta = 43°$), and the 110 planes ($2\theta = 80°$) clearly improved with increasing heat treatment temperature (HTT), which is typical of turbostratic carbon. The full width half maximum (FWHM) values of the XRD 002 and 110 peaks of carbonized wood are shown in Fig. 3. The FWHM values of the XRD 002 and 110 peaks were extracted by Gaussian peaks from the linear-subtracted XRD profiles.[10] The average carbon crystallite thickness (L_c) and the average hexagonal carbon layer diameter (L_a) increased with the decrease of the value of the FWHM of the XRD 002 and 110 peaks, respectively.[10,14,15] A significant decrease of the FWHM of the XRD 002 peak above 1400°C demonstrates increased carbon crystallite thickness. On the other hand, the lateral growth of the hexagonal carbon layer is represented by the decreasing FWHM of the XRD 110 peak below 1400°C. Thus, the XRD results prove the hexagonal carbon layer in carbon crystallites grows in its lateral direction mainly below 1400°C and then the stacking planes in the carbon crystallites increase significantly in the temperature range of 1400° to 1800°C.

The carbon structure was also characterized by micro-Raman spectroscopy. Figure 4 shows the Raman spectra in the range of 1000–1800 cm^{-1} and 900–1300 cm^{-1}.[12] Two Raman bands for carbonized samples were distinctive at 1345–1355 cm^{-1} and 1585–1600 cm^{-1}, corresponding to the in-plane vibrations of sp^2-bonded carbon with structural imperfections (D band for disorder) and the in-plane vibrations of sp^2-bonded crystalline carbon (G band for graphite), respectively.[16] Peaks for a D′ band at 1620 cm^{-1} and for a D″ band in the range 1500–1550 cm^{-1} were also detected in the Raman spectra. The D″ band around 1500–1550 cm^{-1} is associated with an amorphous sp^2-bonded carbon.[17]

The FWHM of the Raman G band for carbonaceous materials was used as a parameter for the estimation of the degree of development of carbon crystallites;[16–18] it becomes narrower with the development of carbon crystallites in carbonaceous materials.[19] Figure 5 shows the FWHM of the Raman G band of carbonized wood, which decreases above 1400°C. On the other hand, the FWHM of the Raman D band, which is related to the degree of disorder of carbon crystallites, also decreased with increased degree of order as shown in Fig. 6.[17,20] The FWHM of the Raman D band decreased with an increase in HTT up to 1400°C. This is due to an increase in the degree of order of carbon crystallites in this HTT range.

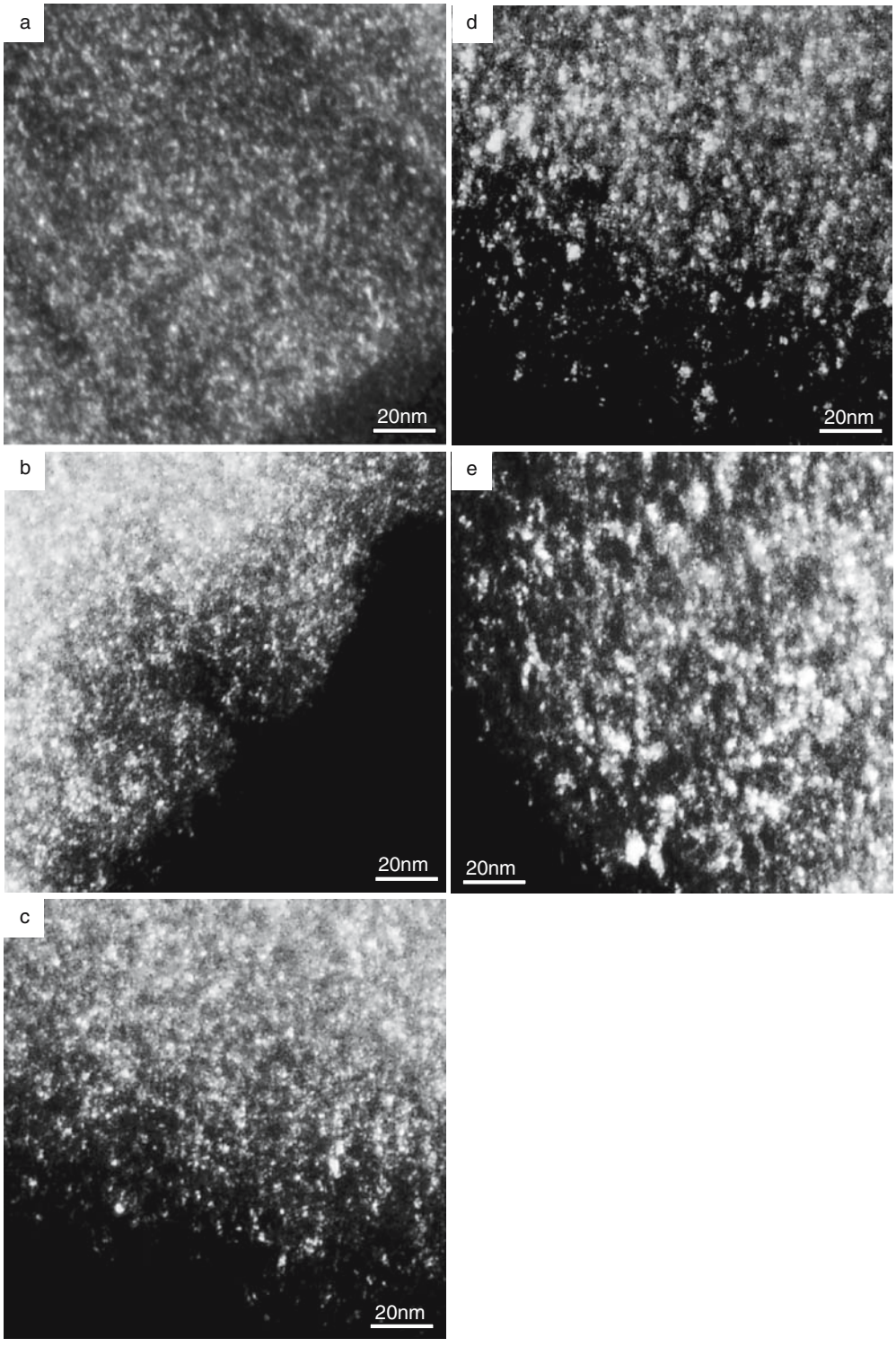

Fig. 1a–e. 002 Dark field (DF) transmission electron microscopy (TEM) images of carbonized wood: **a** 700°C, **b** 1200°C, **c** 1400°C, **d** 1600°C, and **e** 1800°C

Often the intensity ratio of the D″ and G bands ($I_{D''}/I_G$) is used as a parameter for carbonization.[17,21] The relative intensity of the D″ band to the G band decreased remarkably with increasing HTT up to 1400°C (Fig. 7). It shows the reduction of the amorphous phase for sp^2-bonded carbon in this HTT range.

The degree of disorder in carbon crystallites and the amount of the amorphous phase for sp^2-bonded carbons decreased significantly up to 1400°C. The amorphous phase for sp^2-bonded carbon is related to the cross-linking that is an obstacle to the coherent ordering of carbon crystallites. Therefore, the decrease of the amorphous phase for sp^2-bonded carbon allowed the coherent ordering of carbon crystallites in this temperature range. On the other hand, carbon crystallites for sp^2-bonded carbon grew clearly above 1400°C. This could be due to the decomposition of the

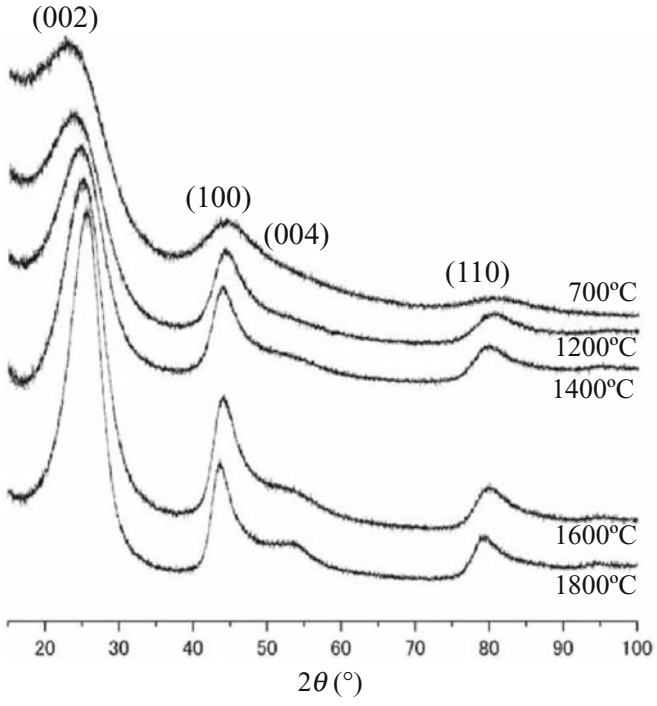

Fig. 2. X-Ray diffraction (XRD) patterns of carbonized wood

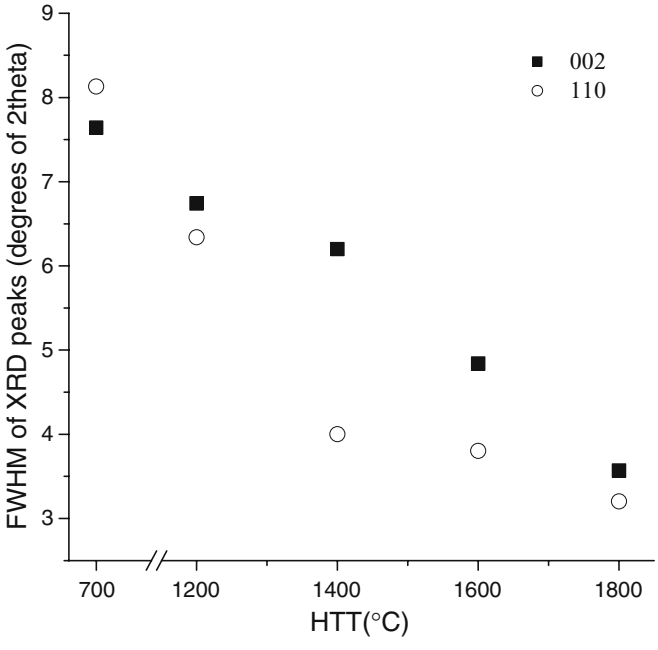

Fig. 3. Full width half maximum (FWHM) of XRD 002 and 110 peaks for carbonized wood. *HTT*, heat treatment temperature

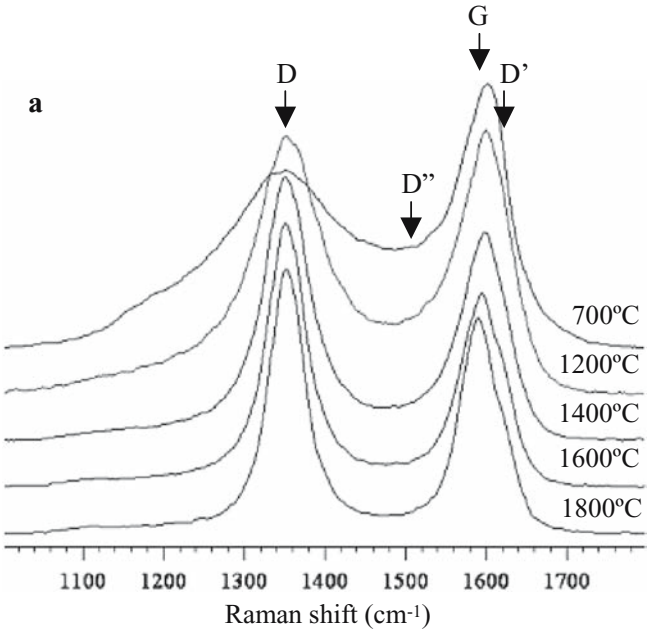

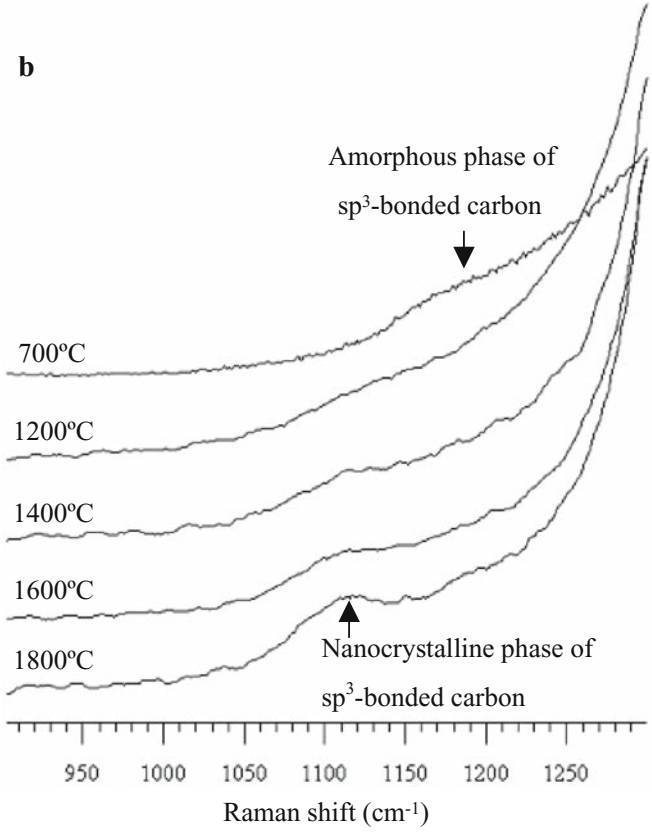

Fig. 4a, b. Raman spectra of carbonized wood for **a** 1000–1800 cm^{-1} and **b** 900–1300 cm^{-1}. Parts of the Raman spectra (700° and 1800°C) are from Ishimaru et al.[12]

cross-links between polyaromatic stacks of ether-type oxygen, amorphous sp^2-bonded carbon, and sp^3-bonded carbon. Thus, the microstructure of carbonized wood changes drastically at around 1400°C.

In addition to these four peaks, the Raman spectra of carbonized wood showed a shoulder or small peak in the range 1120–1190 cm^{-1} as depicted in Fig. 4b, which is assigned to carbon atoms with sp^3-bonded carbon.[18,22–26] In an expansion of the range from 900 to 1300 cm^{-1} from Fig. 4a, Fig. 4b illustrates the extra contribution near 1100 cm^{-1}.

Figure 8 shows the intensity ratio of the sp^3 and G bands (I_{sp3}/I_G) for the heat-treated samples. The relative intensity

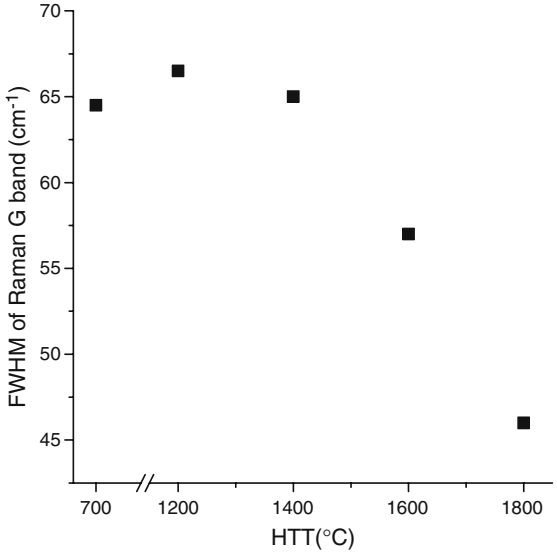

Fig. 5. FWHM of Raman G band for carbonized wood

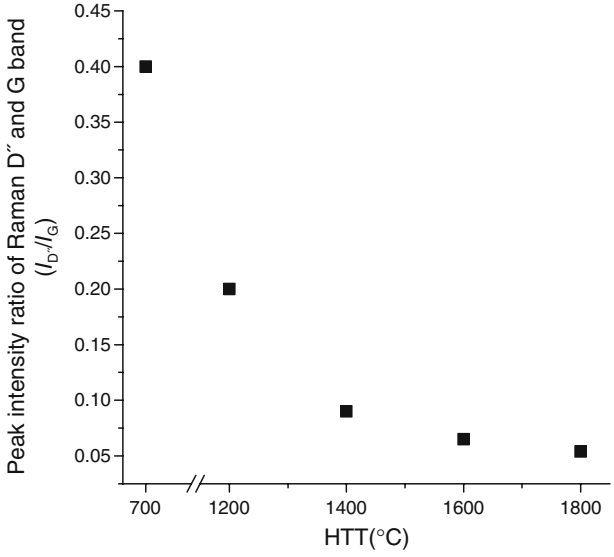

Fig. 7. Peak intensity ratio between Raman D″and G band for carbonized wood

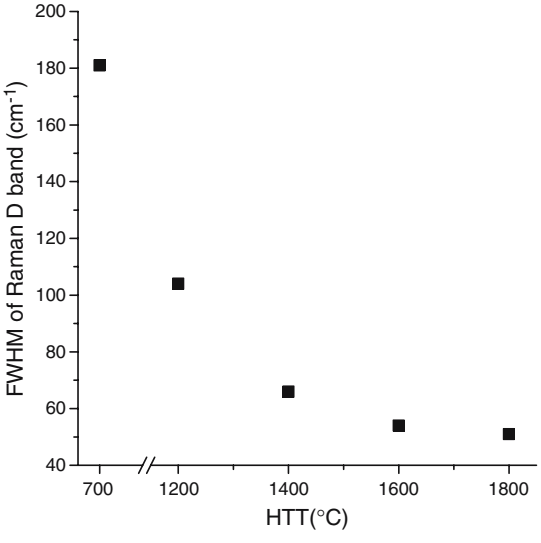

Fig. 6. FWHM of Raman D band for carbonized wood

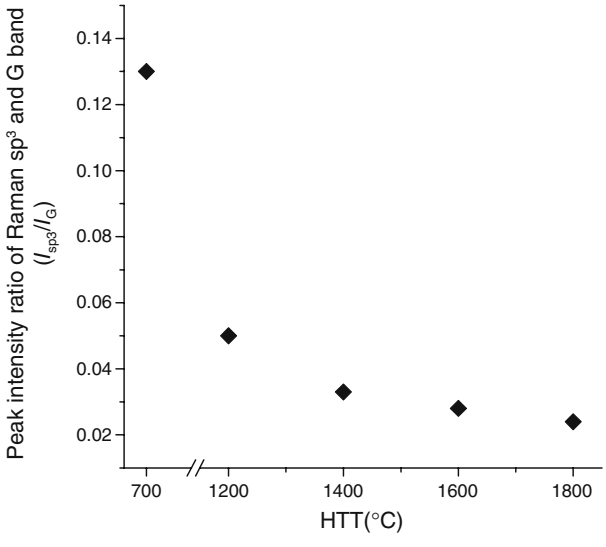

Fig. 8. Peak intensity ratio between Raman sp^3 and G band for carbonized wood

of the sp^3 band to the G band decreased up to 1400°C. From 1400° to 1800°C, an intensity in the sp^3 band was observed that shows the existence of sp^3-bonded carbon in carbonized wood.

At 700°C, the I_{sp3}/I_G value of carbonized wood showed the highest of all HTTs. It has been reported that nanodiamond is formed in wood carbonized at 700°C.[3] However, no peak assigned to the crystalline phase of sp^3-bonded carbon was detected in XRD patterns, as shown in Fig. 2. Therefore, at 700°C, it is considered that most sp^3-bonded carbon in carbonized wood is in an amorphous phase with a small amount in a nanocrystalline phase.

In the Raman spectra of carbonized wood, the shape of a shoulder or small peak, assigned to sp^3-bonded carbon, becomes sharper (Fig. 4b) and the peak position shifted to a lower frequency, from 1190 to 1120 cm^{-1}, with increasing HTT (Fig. 9). It has been reported that a broad peak at about 1250 cm^{-1} could be attributed to amorphous sp^3-bonded carbon.[24] On the other hand, a shoulder or peak in the Raman spectra was often observed in the range 1100–1150 cm^{-1} and was assigned to nanocrystalline diamond (a few nanometers in size).[26] Therefore, it is suggested that the sp^3-bonded carbon transforms from amorphous to nanocrystalline at a HTT range of above 1400°C.

Peaks for sp^2-bonded carbon and a shoulder assigned to sp^3-bonded carbon were observed in the Raman spectra for carbonized wood. It has been reported that sp^3-bonded carbon is present in carbon black and wood charcoal.[3,18] It has also been suggested that the microstructure of nongraphitic carbon is made of sp^2- and sp^3-bonded carbon.[1,2] The

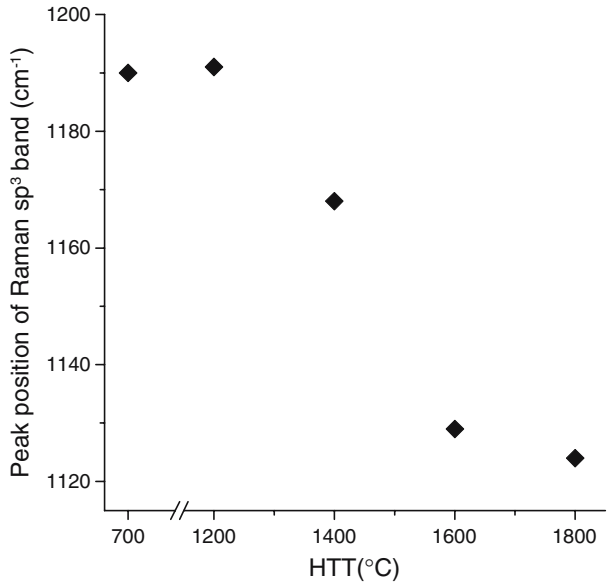

Fig. 9. Peak position of Raman sp^3 band for carbonized wood

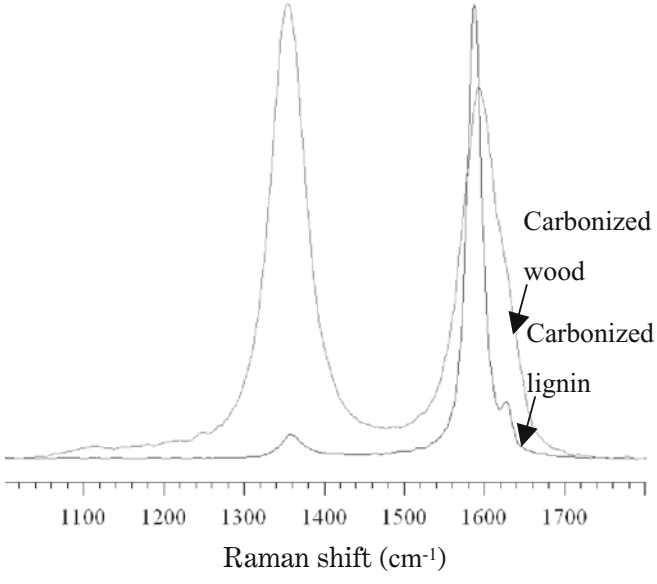

Fig. 10. Raman spectra of carbonized wood and lignin at 1800°C

sp^3-bonded carbon is closely related to the cross-linking between adjacent carbon crystallites.[1] The orientation and growth of carbon crystallites were impeded by the cross-linking between them at temperatures as high as 2000°C.[14] Oxygen-rich and hydrogen-poor carbon precursors such as wood form hard carbon due to the development of cross-linking at the early stages of carbonization.[27,28] The oxygen content of wood is much higher than that of other carbon precursors of hard carbons, which are rich in oxygen, such as lignin, polyfurfuryl alcohol, and phenolic polymers.[28,29] The Raman spectrum of carbonized lignin at 1800°C showed sharp G and D bands and no sp^3 band, as seen in Fig. 10. The FWHM of the Raman G band of carbonized lignin at 1800°C is 21 cm^{-1}, which means that carbonized wood has more disordered carbon crystallites than do other hard carbons such as lignin. Thus, sp^3-bonded carbon develops as cross-links in the microstructure of carbonized wood and disturbs the well-ordered structure of carbon crystallites even at high temperature.

The development behavior of nanocrystalline sp^3-bonded carbon was in good agreement with that of carbon crystallites for sp^2-bonded carbon. When carbon crystallite growth occurs by the movement of groups of crystallites during heat treatment, high internal stresses due to high temperature and pressure conditions are exerted between adjacent carbon crystallites at their edges. High temperature and pressure conditions lead to the formation of the crystalline structure of sp^3-bonded carbons.[30] Therefore, it is suggested that the formation of nanocrystalline sp^3-bonded carbon is closely related to the development of carbon crystallites during heat treatment.

Conclusions

Wood precarbonized at 700°C and subsequently heated to 1800°C by pulse current heating was characterized by TEM, XRD, and micro-Raman spectroscopy. The XRD and TEM results proved that crystalline components of sp^2-bonded carbon develop in carbon crystallites above 1400°C. Thus, the microstructure of carbonized wood changes drastically at about 1400°C. The Raman spectra of carbonized wood showed that part of its microstructure in the HTT range of 700°–1800°C consisted of a combination of sp^2- and sp^3-bonded carbon that is probably due to the highly disordered microstructure of carbonized wood. It is suggested that the sp^3-bonded carbon is transformed from an amorphous state to a nanocrystalline structure with the growth of polyaromatic stacks in a HTT range above 1400°C, which probably shows the development of rigid cross-linking between the carbon crystallites. On the basis of the concerns mentioned above, the microstructure and the properties of carbonized wood could be controlled by adjusting the quantity of sp^3-bonded carbon as cross-links of carbon crystallites.

Acknowledgments The authors are grateful to Prof. Junji Sugiyama, Dr. Fumio Tanaka, and Dr. Masashi Fujisawa, RISH, Kyoto University, for their support in experimental work. This research was carried out with support from Grants-in-Aid for Scientific Research (14002121, 15380119, 18380107) from the Ministry of Education, Culture, Sports, Science and Technology of Japan.

References

1. Kaneko K, Ishii C, Ruike M, Kuwabara H (1992) Origin of superhigh surface area and microcrystalline graphitic structures of activated carbons. Carbon 30:1075–1088
2. Schroder A, Kluppel M, Schuster R, Heidberg J (2002) Surface energy distribution of carbon black measured by static gas adsorption. Carbon 40:207–210
3. Ishimaru K, Vystavel T, Bronsveld P, Hata T, Imamura Y, Hosson JD (2001) Diamond and pore structure observed in wood charcoal. J Wood Sci 47:414–417

4. Hata T, Ishimaru K, Fujisawa M, Bronsveld P, Vystavel T, Hosson JD, Kikuchi H, Nishizawa T, Imamura Y (2005) Catalytic graphitization of wood-based carbons with alumina by pulse current heating. Fullerene Nanotube Carbon Nanostr 13:435–445
5. Greil P, Lifka T, Kaindl A (1998) Biomorphic cellular silicon carbide ceramics from wood I: processing and microstructure. J Eur Ceram Soc 18:1961–1973
6. Fujisawa M, Hata T, Bronsveld P, Castro V, Tanaka F, Kikuchi H, Furuno T, Imamura Y (2004) SiC/C composites from wood charcoal by pulse current sintering with SiO_2 – electrical and thermal properties. J Eur Ceram Soc 24:3575–3580
7. Castro V, Fujisawa M, Hata T, Bronsveld P, Vystavel T, Hosson JD, Kikuchi H, Imamura Y (2004) Silicon carbide nanorods and ceramics from wood. Key Eng Mater 264–268:2267–2270
8. Nishimiya K, Hata T, Imamura Y, Ishihara S (1998) Analysis of chemical structure of wood charcoal by X-ray photoelectron spectroscopy. J Wood Sci 44:56–61
9. Byrne CE, Nagle DC (1997) Carbonized wood monoliths – characterization. Carbon 35:267–273
10. Kercher AK, Nagle DC (2003) Microstructural evolution during charcoal carbonization by X-ray diffraction analysis. Carbon 41:15–27
11. Paris O, Zollfrank C, Zickler G (2005) Decomposition and carbonization of wood biopolymers – a microstructural study of soft wood pyrolysis. Carbon 43:53–66
12. Ishimaru K, Hata T, Bronsveld P, Imamura Y (2007) Microstructural study of carbonized wood after cell wall sectioning. J Mater Sci 42:2662–2668
13. Huttepain H, Oberlin A (1990) Microtexture of nongraphitizing carbons and TEM studies of some activated samples. Carbon 28:103–111
14. Franklin RE (1951) Crystallite growth in graphitizing and nongraphitizing carbons. Proc R Soc A 209:196–218
15. Kobayashi K, Sugawara S, Toyoda S, Honda H (1968) An X-ray diffraction study of phenol-formaldehyde resin carbons. Carbon 6:359–363
16. Katagiri G, Ishida H, Ishitani A (1988) Raman spectra of graphite edge planes. Carbon 26:565–571
17. Jawhari T, Roid A, Casado J (1995) Raman spectroscopic characterization of some commercially available carbon black materials. Carbon 33:1561–1565
18. Pantea D, Darmstadt H, Kaliaguine S, Summchen L, Roy C (2001) Electrical conductivity of thermal carbon blacks: influence of surface chemistry. Carbon 39:1147–1158
19. Darmstadt H, Roy C, Kaliaguine S, Choi SJ, Ryoo R (2002) Surface chemistry of ordered mesoporous carbons. Carbon 40:2673–2683
20. Cuesta A, Dhamelincourt P, Laureyns J, Martinez-Alonso A, Tascon JMD (1994) Raman microprobe studies on carbon materials. Carbon 32:1523–1532
21. Shimodaira N, Masui A (2002) Raman spectroscopic investigations of activated carbon materials. J Appl Phys 92:902–909
22. Schwan J, Ulrich S, Batori V, Ehrhardt H (1996) Raman spectroscopy on amorphous carbon films. J Appl Phys 80:440–447
23. Darmstadt H, Summchen L, Ting JM, Roland U, Kaliaguine S, Roy C (1997) Effects of surface treatment on the bulk chemistry and structure of vapor grown carbon fibers. Carbon 35:1581–1585
24. Prawer S, Nugent KW, Jamieson DN, Orwa JO, Bursill LA, Peng JL (2000) The Raman spectrum of nanocrystalline diamond. Chem Phys Lett 332:93–97
25. Yamauchi S, Kurimoto Y (2003) Raman spectroscopic study on pyrolyzed wood and bark of Japanese cedar: temperature dependence of Raman parameters. J Wood Sci 49:235–240
26. Kromka A, Breza J, Kadlecikova M, Janik J, Balon F (2005) Identification of carbon phases and analysis of diamond/substrate interfaces by Raman spectroscopy. Carbon 43:425–429
27. Oberlin A, Villey M, Combaz A (1980) Influence of elemental composition on carbonization-pyrolysis of kerosene shale and kuckersite. Carbon 18:347–353
28. Ishimaru K, Hata T, Bronsveld P, Imamura Y (2007) Spectroscopic analysis of carbonization behavior of wood, cellulose, and lignin. J Mater Sci 42:122–129
29. Fitzer E, Schafer W (1970) The effect of crosslinking on the formation of glasslike carbons from thermosetting resins. Carbon 8:353–364
30. Yamaoka S, Shaji Kumar MD, Kanda H, Akaishi M (2002) Thermal decomposition of glucose and diamond formation under diamond-stable high pressure-high temperature conditions. Diamond Relat Mater 11:118–124